Quantum Induced Asymmetric Phase Diagrams of Spin-Glass Systems

C. Nadir Kaplan[1] and A. Nihat Berker[1−3]
[1]*Department of Physics, Koç University, Sarıyer 34450, Istanbul, Turkey,*
[2]*Feza Gürsey Research Institute, TÜBITAK - Bosphorus University, Çengelköy 81220, Istanbul, Turkey, and*
[3]*Department of Physics, Massachusetts Institute of Technology, Cambridge, Massachusetts 02139, U.S.A.*

The spin-1/2 quantum Heisenberg model is studied in all spatial dimensions d by renormalization-group theory. Strongly asymmetric phase diagrams in temperature and antiferromagnetic bond probability p are obtained in dimensions $d \geq 3$. The asymmetry at high temperatures approaching the pure ferromagnetic and antiferromagnetic systems disappears as d is increased. However, the asymmetry at low but finite temperatures remains in all dimensions, with the antiferromagnetic phase receding to the ferromagnetic phase. A finite-temperature second-order phase boundary directly between the ferromagnetic and antiferromagnetic phases occurs in $d \geq 6$, resulting in a new multicritical point at its meeting with the boundaries to the paramagnetic phase. In $d = 3, 4, 5$, a paramagnetic phase reaching zero temperature intervenes asymmetrically between the ferromagnetic and reentrant antiferromagnetic phases. There is no spin-glass phase in any dimension.

PACS numbers: 75.10.Nr, 64.60.Ak, 05.45.Df, 05.10.Cc

A conspicuous finite-temperature effect of quantum mechanics is the critical temperature differentiation between ferromagnetic and antiferromagnetic systems.[1, 2, 3, 4] This is a contrast to classical systems where, *e.g.*, on loose-packed lattices ferromagnetic and antiferromagnetic systems are mapped onto each other and therefore have the same critical temperature. We find that this quantum effect is compounded and even more robust in spin-glass systems, which incorporate the passage from ferromagnetism and antiferromagnetism via quenched disorder.

Thus, in the present work, the phase diagrams of the spin-1/2 quantum Heisenberg spin-glass systems are calculated in all dimensions $d \geq 3$. In the space of temperature T and concentration p of antiferromagnetic bonds, remarkably asymmetric phase diagrams are obtained, in very strong contrast to the corresponding classical systems. Whereas, in the limit of $d \to \infty$, the differentiation of the critical temperatures of the ferromagnetic and antiferromagnetic pure systems disappears, the Tp phase diagrams remain strongly asymmetric at low but finite temperatures, where quantum fluctuations remain dominant independent of dimensionality. A direct second-order phase boundary between ferromagnetic and antiferromagnetic phases, also not seen in isotropic classical systems, is found in $d > 5$. In lower d, a paramagnetic phase intervenes between the ferromagnetic and antiferromagnetic systems. Our calculation is an approximation for hypercubic lattices and, simultaneously, a lesser approximation for hierarchical lattices [5, 6, 7, 8, 9, 10, 11, 12, 13, 14, 15].

The spin-1/2 quantum Heisenberg spin-glass systems have the Hamiltonian

$$-\beta\mathcal{H} = \sum_{\langle ij \rangle} J_{ij} \mathbf{s}_i \cdot \mathbf{s}_j \equiv \sum_{\langle ij \rangle} -\beta\mathcal{H}(i,j)\,, \qquad (1)$$

where $\langle ij \rangle$ denotes a sum over pairs of nearest-neighbor sites. J_{ij} is equal to the ferromagnetic value of $J > 0$ with probability $1-p$ and to the antiferromagnetic value of $-J < 0$ with probability p. We solve this model by extending the Suzuki-Takano rescaling [3, 4, 16, 17, 18, 19, 20, 21, 22, 23, 24] to non-uniform systems and to length-rescaling factor $b = 3$, necessary for the *a priori* equivalent treatment of ferromagnetism and antiferromagnetism, followed by the essentially exact treatment [25, 26] of the quenched randomness giving the non-uniformity. In one dimension,

$$\begin{aligned} \mathrm{Tr}_{(j,k)} e^{-\beta\mathcal{H}} &= \mathrm{Tr}_{(j,k)} e^{\sum_i^{4n}\{-\beta\mathcal{H}(i,j)-\beta\mathcal{H}(j,k)-\beta\mathcal{H}(k,l)\}} \\ &\simeq \prod_i^{4n} \mathrm{tr}_{(j,k)} e^{\{-\beta\mathcal{H}(i,j)-\beta\mathcal{H}(j,k)-\beta\mathcal{H}(k,l)\}} \\ &= \prod_i^{4n} e^{-\beta'\mathcal{H}'(i,l)} \simeq e^{\sum_i^{4n}\{-\beta'\mathcal{H}'(i,l)\}} = e^{-\beta'\mathcal{H}'}, \end{aligned} \qquad (2)$$

where the sums and products i are over every fourth spin along the chain, the traces are over all other spins, and $-\beta'\mathcal{H}'$ is the renormalized Hamiltonian. Thus, the commutation rules are correctly accounted for within four-site segments, at all successive length scales in the iterations of the renormalization-group transformation. The trace tr is performed by quantum algebra, as given in the Appendix.

The rescaling is extended to dimensions $d > 1$ by bond-moving, namely by adding b^{d-1} interactions resulting from the decimation of Eq.(2), to obtain the renormalized interaction strength $J'_{i'j'} = R(\{J_{ij}\})$, where $\{J_{ij}\}$ includes b^d interactions of the unrenormalized system. The interaction constant values $\{J_{ij}\}$ are distributed with a quenched probability distribution $\mathcal{P}(J_{ij})$ [25, 26], which starts out as a double-delta function as described after Eq.(1) but quickly becomes complicated under its renormalization-group transformation, given by the convolution

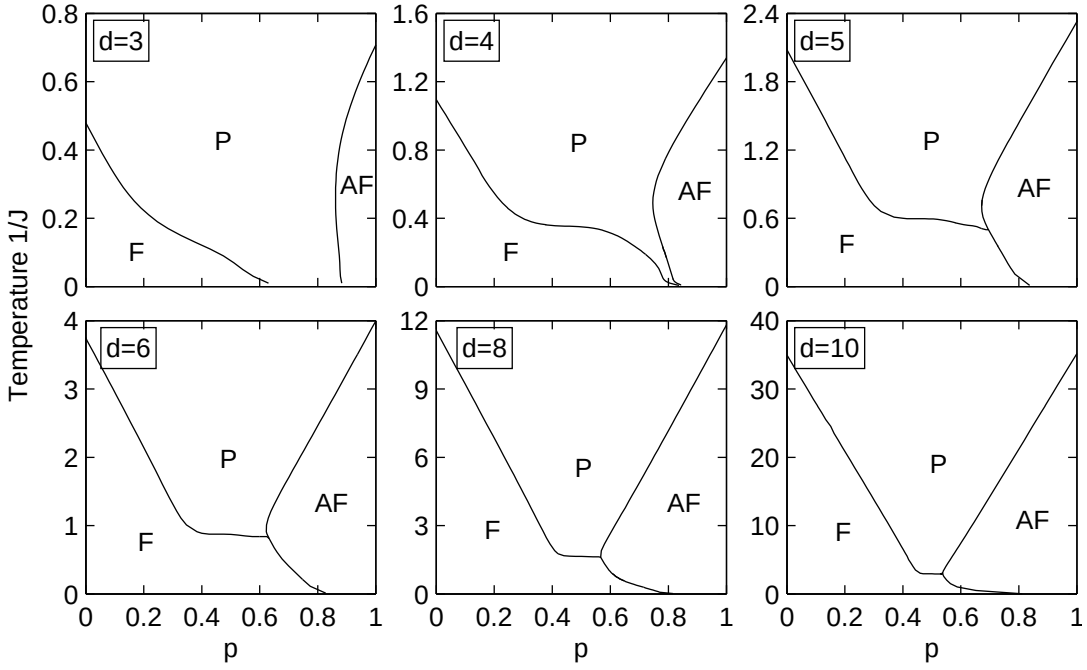

FIG. 1: Phase diagrams of the quantum Heisenberg spin-glass systems in temperature $1/J$ versus antiferromagnetic bond concentration p for $d = 3$ to 10. All transitions are second-order, between the ferromagnetic (F), antiferromagnetic(AF), and paramagnetic (P) phases.

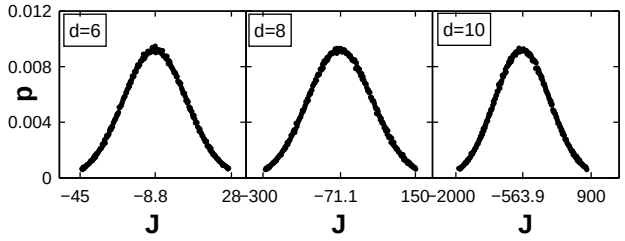

FIG. 2: Unstable fixed distributions that control the finite-temperature phase boundary between the ferromagnetic and antiferromagnetic phases. For the purpose of this figure, an equal-interval binning of 40,000 histograms has been done.

$$\mathcal{P}'(J'_{i'j'}) = \int \left[\prod_{ij}^{i'j'} dJ_{ij}\, \mathcal{P}(J_{ij}) \right] \delta\left(J'_{i'j'} - R(\{J_{ij}\}) \right) . \tag{3}$$

This equation actually involves b^d convolutions (for example, 729 convolutions for the $d = 6$ system discussed below), which are constituted of triplet convolutions of interactions in series (decimation) and pairwise convolutions of interactions in parallel (bond-moving). The quenched probability distribution $\mathcal{P}(J_{ij})$ is kept numerically in terms of histograms. The number of histograms multiplicatively increases under rescaling, until a calculationally acceptable maximum is reached. After this point, the number of histograms is kept constant by implementing a binning procedure before each pairwise or triplet convolution. We employ a new binning procedure, in which bins are demarked so as to contain equal probabilities, as opposed to equal interaction intervals as done previously. Starting from the lowest J value and moving to greater ones, histograms in each consecutive bin are combined, to interaction value $J = \Sigma p_i J_i / \Sigma p_i$ and imposed equal probability $p = \Sigma p_i = 1/n_{\rm bin}$. In this process, histograms at the boundaries of bins are apportioned between the consecutive bins. This binning method is clearly independent of direction, that is, starting from the greatest J value and moving to lower ones results in the same binned probability distribution. Thus, our calculation has 125,000 histograms after each decimation and 40,000 histograms after each pairwise bond moving. The global flows of the quenched probability distributions yield the phase diagrams. Analysis of the unstable fixed points and unstable fixed distributions attracting the phase boundaries yields the order of the phase transitions.

Calculations are done for the quantum Heisenberg spin-glass systems in integer dimensions. No finite-temperature phase transition occurs in $d = 1, 2$. The phase diagrams for $d = 3, 4, 5, 6, 8, 10$ are shown in Fig.1. They are all strikingly asymmetric, especially in the middle p and low-temperature (would-be spin-glass phase) region. In $d = 3$, our calculated ratio of the critical temperatures of the pure antiferromagnetic and ferromagnetic systems is $T_C^{AF}/T_C^F = 1.48$. This value is to be compared with the values of 1.13 found in the cubic lattice [1, 2] and 1.22 found in the $b = 2, d = 3$ hierarchical lattice [3, 4]. This critical temperature difference

is consistent with the lower ground-state energy of the antiferromagnetic system, as calculated [27] in $d = 3$. Our calculated ratios of the antiferromagnetic and ferromagnetic critical temperatures, for $d = 4, 5, 6, 8, 10$, decrease as 1.22, 1.12, 1.07, 1.02, 1.01 respectively. On the other hand, it is seen that although the phase boundaries leading to the pure ferromagnetic and antiferromagnetic critical points regain symmetry as d is increased, the low-temperature phase diagrams remain asymmetric. The ferromagnetic phase penetrates the antiferromagnetic region at low temperatures. Thus, quantum fluctuations present at low temperatures favor the ferromagnetic phase over the antiferromagnetic phase. In $d \geq 6$, a second-order phase boundary occurs directly between the ferromagnetic and antiferromagnetic phases, as is not seen in isotropic classical spin-glass systems. This phase boundary is controlled by the unstable fixed distributions shown in Fig.2. A new multicritical point occurs where all three second-order boundaries meet. In $d = 3, 4, 5$, the paramagnetic phase reaching zero temperature (as an extremely narrow sliver in $d = 5$) intervenes between the ferromagnetic and antiferromagnetic phases. In all cases, the ferromagnetic phase penetrates, reaching the high p values of 0.63 and 0.83 respectively in $d = 3$, where there is a zero-temperature paramagnetic interval, and $d \geq 4$, where there is no zero-temperature paramagnetic interval. The antiferromagnetic phase recedes at low temperatures, thereby showing a reentrant phase boundary [26].

There is no spin-glass phase, in the quantum system, in any dimension. The quantum version of the Sherrington-Kirkpatrick model [28], namely the spin-1/2 quantum Heisenberg model with equivalent-neighbor interactions, with a symmetric gaussian distribution, studied from the high-temperature side, yields a finite-temperature phase transition, which has been interpreted as a transition to a low-temperature spin-glass phase [29]. This model should be similar to our studied models at $p = 0.5$ in the large d limit. Thus, we also find a finite-temperature phase transition (Fig.1), but the low-temperature phase is explicitly a ferromagnetic phase with quenched bond randomness. The latter phase has considerable amount of short-range antiferromagnetic correlations, as seen in Ref.[30].

Acknowledgments

We are grateful to M. Hinczewski and H. Nishimori for useful comments. This research was supported by the Scientific and Technical Research Council (TÜBİTAK) and by the Academy of Sciences of Turkey.

APPENDIX A: QUANTUM RECURSION RELATIONS

The operators $-\beta'\mathcal{H}'(i,l)$ and $-\beta\mathcal{H}(i,j) - \beta\mathcal{H}(j,k) - \beta\mathcal{H}(k,l)$ of Eq. (2) act on two-site and four-site states, respectively, where at each site the spin is in quantum state $\sigma = \uparrow$ or $\downarrow$. The trace tr in Eq. (2) is, in terms of matrix elements [3],

$$\langle u_i z_l | e^{-\beta'\mathcal{H}'(i,l)} | \bar{u}_i \bar{z}_l \rangle = \sum_{v_j, w_k} \langle u_i\, v_j\, w_k\, z_l | e^{-\beta\mathcal{H}(i,j) - \beta\mathcal{H}(j,k) - \beta\mathcal{H}(k,l)} | \bar{u}_i\, v_j\, w_k\, \bar{z}_l \rangle \,, \tag{A1}$$

where $u_i, v_j, w_k, z_l, \bar{u}_i, \bar{z}_l$ are single-site state variables. Thus, Eq. (A1) is the contraction of a 16×16 matrix into a 4×4 matrix. Basis states that are simultaneous eigenstates of parity (p), total spin magnitude (s), and total spin z-component (m_s) block-diagonalize these matrices and thereby make Eq. (A1) manageable. These sets of 4 two-site and 16 four-site eigenstates, denoted by $\{|\phi_p\rangle\}$ and $\{|\psi_q\rangle\}$ respectively, are given in Tables I and II. The diagonal blocks are given in Tables III and IV. Due to the microscopic randomness of the spin-glass problem, the four-site Hamiltonian mixes states of differ-

p	s	m_s	Two-site eigenstates
+	1	1	$\|\phi_1\rangle = \|\uparrow\uparrow\rangle$
+	1	0	$\|\phi_2\rangle = \frac{1}{\sqrt{2}}\{\|\uparrow\downarrow\rangle + \|\downarrow\uparrow\rangle\}$
−	0	0	$\|\phi_4\rangle = \frac{1}{\sqrt{2}}\{\|\uparrow\downarrow\rangle - \|\downarrow\uparrow\rangle\}$

TABLE I: The two-site basis states, with the corresponding parity (p), total spin (s), and total spin z-component (m_s) quantum numbers. The state $|\phi_3\rangle$ is obtained by spin reversal from $|\phi_1\rangle$.

p	s	m_s	Four-site eigenstates
+	2	2	$\|\psi_1\rangle = \|\uparrow\uparrow\uparrow\uparrow\rangle$
+	2	1	$\|\psi_2\rangle = \frac{1}{2}\{\|\uparrow\uparrow\uparrow\downarrow\rangle + \|\uparrow\uparrow\downarrow\uparrow\rangle + \|\uparrow\downarrow\uparrow\uparrow\rangle + \|\downarrow\uparrow\uparrow\uparrow\rangle\}$
+	2	0	$\|\psi_3\rangle = \frac{1}{\sqrt{6}}\{\|\uparrow\uparrow\downarrow\downarrow\rangle + \|\uparrow\downarrow\uparrow\downarrow\rangle + \|\uparrow\downarrow\downarrow\uparrow\rangle + \|\downarrow\uparrow\uparrow\downarrow\rangle + \|\downarrow\uparrow\downarrow\uparrow\rangle + \|\downarrow\downarrow\uparrow\uparrow\rangle\}$
+	1	1	$\|\psi_6\rangle = \frac{1}{2}\{\|\uparrow\uparrow\uparrow\downarrow\rangle - \|\uparrow\uparrow\downarrow\uparrow\rangle - \|\uparrow\downarrow\uparrow\uparrow\rangle + \|\downarrow\uparrow\uparrow\uparrow\rangle\}$
+	1	0	$\|\psi_7\rangle = \frac{1}{\sqrt{2}}\{\|\downarrow\uparrow\uparrow\downarrow\rangle - \|\uparrow\downarrow\downarrow\uparrow\rangle$
−	1	1	$\|\psi_9\rangle = \frac{1}{2}\{\|\uparrow\uparrow\uparrow\downarrow\rangle - \|\uparrow\uparrow\downarrow\uparrow\rangle + \|\uparrow\downarrow\uparrow\uparrow\rangle - \|\downarrow\uparrow\uparrow\uparrow\rangle\}$ $\|\psi_{10}\rangle = \frac{1}{2}\{\|\uparrow\uparrow\uparrow\downarrow\rangle + \|\uparrow\uparrow\downarrow\uparrow\rangle - \|\uparrow\downarrow\uparrow\uparrow\rangle - \|\downarrow\uparrow\uparrow\uparrow\rangle\}$
−	1	0	$\|\psi_{11}\rangle = \frac{1}{\sqrt{2}}\{\|\uparrow\downarrow\uparrow\downarrow\rangle - \|\downarrow\uparrow\downarrow\uparrow\rangle$ $\|\psi_{12}\rangle = \frac{1}{\sqrt{2}}\{\|\uparrow\uparrow\downarrow\downarrow\rangle - \|\downarrow\downarrow\uparrow\uparrow\rangle$
+	0	0	$\|\psi_{15}\rangle = \frac{1}{2}\{\|\uparrow\uparrow\downarrow\downarrow\rangle - \|\uparrow\downarrow\uparrow\downarrow\rangle - \|\downarrow\uparrow\downarrow\uparrow\rangle + \|\downarrow\downarrow\uparrow\uparrow\rangle\}$ $\|\psi_{16}\rangle = \frac{1}{\sqrt{12}}\{\|\uparrow\uparrow\downarrow\downarrow\rangle + \|\uparrow\downarrow\uparrow\downarrow\rangle - 2\|\uparrow\downarrow\downarrow\uparrow\rangle$ $-2\|\downarrow\uparrow\uparrow\downarrow\rangle + \|\downarrow\uparrow\downarrow\uparrow\rangle + \|\downarrow\downarrow\uparrow\uparrow\rangle\}$

TABLE II: The four-site basis states, with the corresponding parity (p), total spin (s), and total spin z-component (m_s) quantum numbers. The states $|\psi_{4,5}\rangle$, $|\psi_8\rangle$, $|\psi_{13,14}\rangle$ are obtained by spin reversal from $|\psi_{2,1}\rangle$, $|\psi_6\rangle$, $|\psi_{9,10}\rangle$, respectively.

	ϕ_1	ϕ_4
ϕ_1	$\frac{1}{4}J' + G'$	
ϕ_4		$-\frac{3}{4}J' + G'$

TABLE III: Block-diagonal matrix of the renormalized two-site Hamiltonian $-\beta' H'(i,l)$. The diagonal elements of $|\phi_2\rangle$ and $|\phi_3\rangle$ are equal to that of $|\phi_1\rangle$.

	ψ_1	ψ_2	ψ_3
ψ_1	$\frac{1}{4}(J_1+J_2+J_3)$	0	0
ψ_2	0	$\frac{1}{4}(J_1+J_2+J_3)$	0
ψ_3	0	0	$\frac{1}{4}(J_1+J_2+J_3)$

	ψ_6	ψ_9	ψ_{10}
ψ_6	$\frac{1}{4}(-J_1+J_2-J_3)$	$\frac{1}{2}(J_1-J_3)$	0
ψ_9	$\frac{1}{2}(J_1-J_3)$	$-\frac{1}{4}(J_1+J_2+J_3)$	$\frac{1}{2}J_2$
ψ_{10}	0	$\frac{1}{2}J_2$	$\frac{1}{4}(J_1-J_2+J_3)$

	ψ_7	ψ_{11}	ψ_{12}
ψ_7	$\frac{1}{4}(-J_1+J_2-J_3)$	$\frac{1}{2}(J_1-J_3)$	0
ψ_{11}	$\frac{1}{2}(J_1-J_3)$	$-\frac{1}{4}(J_1+J_2+J_3)$	$\frac{1}{2}J_2$
ψ_{12}	0	$\frac{1}{2}J_2$	$\frac{1}{4}(J_1-J_2+J_3)$

	ψ_{15}	ψ_{16}
ψ_{15}	$-\frac{3}{4}J_2$	$\frac{\sqrt{3}}{4}(J_1+J_3)$
ψ_{16}	$\frac{\sqrt{3}}{4}(J_1+J_3)$	$\frac{1}{4}(-2J_1+J_2-2J_3)$

TABLE IV: Diagonal matrix blocks of the unrenormalized three-site Hamiltonian $-\beta H(i,j)-\beta H(j,k)-\beta H(k,l)$. The Hamiltonian being invariant under spin-reversal, the spin-flipped matrix elements are not shown. The interaction constants J_1, J_2, J_3, which are in general unequal due to quenched randomness, are from $-\beta\mathcal{H}(i,j), -\beta\mathcal{H}(j,k), -\beta\mathcal{H}(k,l)$ respectively.

ent parity, as seen in Table IV. Eq. (A1) is thus rewritten as

$$\langle\phi_p|e^{-\beta'\mathcal{H}'(i,k)}|\phi_{\bar{p}}\rangle = \sum_{\substack{u,z,\bar{u},\\ \bar{z},v,w}}\sum_{q,\bar{q}}\langle\phi_p|u_i z_l\rangle\langle u_i v_j w_k z_l|\psi_q\rangle \langle\psi_q|e^{-\beta\mathcal{H}(i,j)-\beta\mathcal{H}(j,k)-\beta\mathcal{H}(k,l)}|\psi_{\bar{q}}\rangle\langle\psi_{\bar{q}}|\bar{u}_i v_j w_k \bar{z}_l\rangle\langle\bar{u}_i\bar{z}_l|\phi_{\bar{p}}\rangle. \tag{A2}$$

There are only two rotation-symmetry independent elements of $\langle\phi_p|e^{-\beta'\mathcal{H}'(i,l)}|\phi_{\bar{p}}\rangle \equiv \langle\phi_p||\phi_{\bar{p}}\rangle$ in Eq.(A2), which have $p=\bar{p}=1,4$ (thereby leading to one renormalized interaction constant J' and the additive constant G'). From Eq. (A2),

$$\langle\phi_1||\phi_1\rangle = \langle\psi_1||\psi_1\rangle + \frac{1}{2}\langle\psi_2||\psi_2\rangle + \frac{1}{6}\langle\psi_3||\psi_3\rangle + \frac{1}{2}\langle\psi_6||\psi_6\rangle + \frac{1}{2}\langle\psi_7||\psi_7\rangle + \frac{1}{2}\langle\psi_9||\psi_9\rangle - \langle\psi_9||\psi_{10}\rangle + \frac{1}{2}\langle\psi_{10}||\psi_{10}\rangle + \frac{1}{3}\langle\psi_{16}||\psi_{16}\rangle\,,$$

$$\langle\phi_4||\phi_4\rangle = \langle\psi_9||\psi_9\rangle + 2\langle\psi_9||\psi_{10}\rangle + \langle\psi_{10}||\psi_{10}\rangle + \frac{1}{2}\langle\psi_{11}||\psi_{11}\rangle + \langle\psi_{11}||\psi_{12}\rangle + \frac{1}{2}\langle\psi_{12}||\psi_{12}\rangle + \langle\psi_{15}||\psi_{15}\rangle\,,$$

where $\langle\psi_q||\psi_{\bar{q}}\rangle \equiv \langle\psi_q|e^{-\beta\mathcal{H}(i,j)-\beta\mathcal{H}(j,k)-\beta\mathcal{H}(k,l)}|\psi_{\bar{q}}\rangle$. From Table III, the renormalized interaction constant is given by $J' = \ln(\langle\phi_1||\phi_1\rangle/\langle\phi_4||\phi_4\rangle)$.

[1] G.S. Rushbrooke and P.J. Wood, Mol. Phys. **6**, 409 (1963).
[2] J. Oitmaa and W. Zheng, J. Phys.: Condens. Matter **16**, 8653 (2004).
[3] A. Falicov and A.N. Berker, Phys. Rev. B **51**, 12458 (1995).
[4] M. Hinczewski and A.N. Berker, Eur. Phys. J. B **48**, 1 (2005).
[5] A.N. Berker and S. Ostlund, J. Phys. C **12**, 4961 (1979).
[6] R.B. Griffiths and M. Kaufman, Phys. Rev. B **26**, 5022R (1982).
[7] M. Kaufman and R.B. Griffiths, Phys. Rev. B **30**, 244 (1984).
[8] A. Erbaş, A. Tuncer, B. Yücesoy, and A.N. Berker, Phys. Rev. E **72**, 026129 (2005).
[9] M. Hinczewski and A.N. Berker, Phys. Rev. E **73**, 066126 (2006).
[10] M. Hinczewski, Phys. Rev E **75**, 061104 (2007).
[11] Z. Zhang, L. Rong, and S. Zhou, Physica A **377**, 329 (2007).
[12] Z. Zhang, S. Zhou, and T. Zou, Eur. Phys. J. B **56**, 259 (2007).
[13] H.D. Rozenfeld and D. ben-Avraham, Phys. Rev. E **75**, 061102 (2007).
[14] H.D. Rozenfeld, S. Havlin, and D. ben-Avraham, New J. Phys. **9**, 175 (2007).
[15] E. Khajeh, S.N. Dorogovtsev, and J.F.F. Mendes, Phys. Rev. E **75**, 041112 (2007).
[16] M. Suzuki and H. Takano, Phys. Lett. A **69**, 426 (1979).
[17] H. Takano and M. Suzuki, J. Stat. Phys. **26**, 635 (1981).
[18] P. Tomczak, Phys. Rev. B **53**, R500 (1996).
[19] P. Tomczak and J. Richter, Phys. Rev. B **54**, 9004 (1996).
[20] P. Tomczak and J. Richter, J. Phys. A **36**, 5399 (2003).
[21] M. Hinczewski and A.N. Berker, Eur. Phys. J. B **51**, 461 (2006).
[22] M. Hinczewski and A.N. Berker, cond-mat/0607171.
[23] C.N. Kaplan, A.N. Berker, and M. Hinczewski, preprint (2007).
[24] O.S. Sarıyer, A.N. Berker and M. Hinczewski, arXiv:0704.1064v1 [cond-mat.stat-mech].
[25] A. Falicov, A.N. Berker, and S.R. McKay, Phys. Rev. B **51**, 8266 (1995).

[26] G. Migliorini and A.N. Berker, Phys. Rev. B **57**, 426 (1998).
[27] H. Nishimori and S.J. Miyake, Prog. Theor. Phys. **73**, 18 (1985).
[28] D. Sherrington and S. Kirkpatrick, Phys. Rev. Lett. **32**, 1792 (1975).
[29] A.J. Bray and M.A. Moore, J. Phys. C **13**, L655 (1980).
[30] B. Yücesoy and A.N. Berker, Phys. Rev. B **76**, 014417 (2007).